

This Prospectus for a Dissertation
entitled
PLASMA FLOW CONTROL
FOR NOISE REDUCTION
ON A G550 NOSE LANDING GEAR

typeset with $\text{NDDiss2}_{\mathcal{E}}$ v3.2013 (2013/04/16) on December 8, 2015 for

Michael C. Wicks

This $\text{\LaTeX} 2_{\mathcal{E}}$ classfile conforms to the University of Notre Dame style guidelines as of Fall 2012. However it is still possible to generate a non-conformant document if the instructions in the class file documentation are not followed!

Be sure to refer to the published Graduate School guidelines at <http://graduateschool.nd.edu> as well. Those guidelines override everything mentioned about formatting in the documentation for this $\text{NDDiss2}_{\mathcal{E}}$ class file.

It is YOUR responsibility to ensure that the Chapter titles and Table caption titles are put in CAPS LETTERS. This classfile does *NOT* do that!

*This page can be disabled by specifying the “noinfo” option to the class invocation.
(i.e., \documentclass[. . . , noinfo] {nddiss2e})*

This page is *NOT* part of the dissertation/thesis. It should be disabled before making final, formal submission, but should be included in the version submitted for format check.

$\text{NDDiss2}_{\mathcal{E}}$ documentation can be found at these locations:

<http://www.gsu.nd.edu>
<http://graduateschool.nd.edu>

PLASMA FLOW CONTROL
FOR NOISE REDUCTION
ON A G550 NOSE LANDING GEAR

A Prospectus for a Dissertation

Submitted to the Graduate School
of the University of Notre Dame
in Partial Fulfillment of the Requirements
for the Degree of

Doctor of Philosophy

by
Michael C. Wicks

Flint O. Thomas, Director

Graduate Program in Aerospace and Mechanical Engineering

Notre Dame, Indiana

December 2015

© Copyright by
Michael C. Wicks
2015
All Rights Reserved

PLASMA FLOW CONTROL
FOR NOISE REDUCTION
ON A G550 NOSE LANDING GEAR

Abstract

by

Michael C. Wicks

Please note that the full \LaTeX source code (and an associated `Makefile`) is available from the University of Notre Dame Graduate Student Union web site. The Information Technology Committee page¹ has all the necessary files in download-able form. This particular dissertation was developed under Unix, but is also be usable under Windows with the appropriate \LaTeX setup and was modified on a Windows system in 2012-2013. It should also work with on Mac.

While the source code for this document provides an excellent example for how to use the `NDdiss2 ε` \LaTeX class to write a Notre Dame thesis, it is *not* a substitution for the documentation of the `NDdiss2 ε` \LaTeX class (also available on the ND GSU web site).

In this thesis, I will tell all that I know about Gnus. Gnus are wonderful little creatures that inhabit the center of the earth and give us wonderful and plentiful trees, dirt, and other earthly-things.

In short, we should love and cherish the Gnus. They can be very friendly, and are often mistaken for squirrels on the University of Notre Dame campus. Feed them

¹<http://www.gsu.nd.edu/>

whenever possible. If they get caught in trash cans, tip them over so that they can get out.

This abstract is going to continue on, including a few formulas, just for the sake of spilling over on to two pages so that we can see the author's name in the top right corner:

$$a^2 + b^2 = c^2$$

$$E = mc^2$$

$$\frac{e}{m} = c^2$$
$$a^2 + b^2 = \frac{e}{m}$$

These equations, by themselves mean nothing. But to the common Gnu, they define a whole way of living. While intricate mathematical implications certainly do not infiltrate the majority of humans' lives, every Gnu, from birth, is imbued with a sense of mathematical certainty and guidance. All Gnus, great and small, feel at one with mathematics. The cute furry bit is just a scam for their calculating minds.

To Laurimar

CONTENTS

FIGURES	v
TABLES	vi
CHAPTER 1: INTRODUCTION	1
1.1 Motivation	1
1.2 Theory of Aeroacoustics	1
1.3 Landing Gear	6
1.3.1 Geometry	6
1.3.2 Noise Sources	6
1.4 Literature Review	6
1.4.1 Single Cylinder Plasma Flow Control	6
1.4.2 Tandem Cylinders Plasma Flow Control	6
1.4.3 Shock Strut-Torque Arm Assembly Plasma Flow Control	6
CHAPTER 2: EXPERIMENTAL APPROACH	9
2.1 Experimental Objective	9
2.2 Experimental Facility	9
2.3 Notre Dame G550 Nose Landing Gear Model	9
2.4 Flow Visualization	11
2.5 Pressure Measurements	11
2.6 Microphone Measurements	11
2.7 Data Acquisition	11
2.8 Current Results	13
2.8.1 Wind Tunnel Background Noise Characterization	13
2.8.2 Far field check	13
2.8.3 Effects of Tripping	16
2.8.4 Comparison with University of Florida Anechoic Flow Facility Measurements	16
2.8.5 Baseline Sound Magnitude and Directivity	18
CHAPTER 3: OBJECTIVES AND FUTURE WORK	25
3.1 Research Objectives	25
3.2 Proposed Future Work	25
3.3 Conclusion	25

BIBLIOGRAPHY	26
------------------------	----

FIGURES

1.1	Photograph of Gulfstream 550 Nose Landing Gear	4
1.2	Schematic view of Gulfstream 550 Nose Landing Gear components . .	5
1.3	Flow Visualization of single cylinder in cross-flow with Spanwise and PSVG plasma actuators.	6
1.4	Flow Visualization of tandem cylinders in cross-flow with Spanwise and PSVG plasma actuators.	7
1.5	Flow Visualization of torque-arm assembly in cross-flow with Spanwise plasma actuators.	8
2.1	ND G550 model with and without plasma fairing installed.	10
2.2	Schematic of the polar array.	12
2.3	Photograph of the polar array installed in the ND AWT.	12
2.4	Representative far field noise level with and without Baseline 1 model installed at $\theta = 90^\circ$	14
2.5	Representative far field noise level with and without Baseline 1 model installed at $\theta = 90^\circ$	15
2.6	Comparison of far field noise level with and without the presence of a trip at $\theta = 90^\circ$	17
2.7	Comparison of far field noise level at UFAFF and ND AWT facilities at $\theta = 90^\circ$	19
2.8	Comparison of design of the NASA G550 and ND G550 model geometries.	19
2.9	1/3-octave band SPL	21
2.10	1/3-octave band SPL	22
2.11	Polar plot	23
2.12	Landing Gear Flow Visualization	24

TABLES

2.1 Data acquisition parameters. 13

CHAPTER 1

INTRODUCTION

Airframe noise is significant

Landing gear is primary source of airframe noise

Health risks

1.1 Motivation

The present work is motivated to reduce noise by flow control via application of DBD plasma actuator technology.

In this chapter, the physics of airframe noise production is discussed. The structure of Aircraft landing gear is presented. This geometry is grouped into two main sub-systems which can be considered for flow-control separately. Areas of noise contribution are considered and the underlying physical mechanisms are discussed. Finally, the literature is reviewed with respect to the application of Plasma Flow Control to increasingly complex geometries.

1.2 Theory of Aeroacoustics

The modern theory of aeroacoustics, that is sound generated by aerodynamic means, is based on James Lighthill's so-called acoustic analogy. He states that sound generated in a fluid flow is only important in regions of turbulent fluctuations [1]. Based on this assumption, the Navier-Stokes Equation and isentropic equation of state are

$$\frac{\partial \rho}{\partial t} + \frac{\partial(\rho u_i)}{\partial x_i} = 0 \quad (1.1)$$

$$\frac{\partial(\rho u_i)}{\partial t} + \frac{\partial(\rho u_i u_j + P_{ij})}{\partial x_j} = 0 \quad (1.2)$$

$$c_o^2 = \frac{\partial p}{\partial \rho}|_{s=const.} = \frac{p'}{\rho'}. \quad (1.3)$$

$$\frac{\partial^2 \rho}{\partial t^2} - c_o^2 \nabla^2 \rho = \frac{\partial^2 T_{ij}}{\partial x_i \partial x_j}. \quad (1.4)$$

$$T_{ij} = \rho u_i u_j + P_{ij} - c_o^2 (\rho - \rho_0) \delta_{ij}, \quad (1.5)$$

where

$$\delta_{ij} = \begin{cases} 1 & \text{if } i = j \\ 0 & \text{if } i \neq j \end{cases} \quad (1.6)$$

$$T_{ij} \approx \rho_0 u_i u_j. \quad (1.7)$$

$$p' = c_o^2 \rho' = \frac{1}{4\pi} \frac{\partial^2}{\partial x_i \partial x_j} \int_V \frac{T_{ij}}{r} dV, \quad (1.8)$$

$$\int_V dV \propto D^3 \quad (1.9)$$

$$T_{ij} \propto \rho_o U_o^2 \quad (1.10)$$

$$\frac{\partial}{\partial x_i} = \frac{\partial}{c_o \partial t} \propto \frac{f}{c_o} \propto \frac{U_o}{c_o D} \quad (1.11)$$

$$p' \propto \left(\frac{U_o}{c_o D} \right)^2 (D^3) \left(\frac{\rho_o U_o^2}{r} \right) \propto \frac{U_o^4}{r} \quad (1.12)$$

$$W \propto p'^2 \propto \frac{U_o^8}{r^2} \quad (1.13)$$

$$\begin{aligned} p' = & \underbrace{\frac{1}{4\pi} \frac{\partial^2}{\partial x_i \partial x_j} \int_V \left[\frac{T_{ij}}{r} \right] dV}_{I} - \underbrace{\frac{1}{4\pi} \frac{\partial}{\partial x_j} \int_S \left[\frac{P_{ij} + \rho v_i v_j}{r} \right] n_i dS}_{II} \\ & + \underbrace{\frac{1}{4\pi} \frac{\partial}{\partial t} \int_S \left[\frac{\rho v_i}{r} \right] n_i dS}_{III}, \end{aligned} \quad (1.14)$$

$$II : \frac{1}{4\pi} \frac{\partial}{\partial x_j} \int_S \left[\frac{P_{ij} + \rho v_i v_j}{r} \right] n_i dS \propto \left(\frac{U_o}{c_o D} \right) \left(\frac{\rho_o U_o^2}{r} \right) (D^2) \propto \frac{U_o^3}{r} \quad (1.15)$$

$$III : \frac{1}{4\pi} \frac{\partial}{\partial t} \int_S \left[\frac{\rho v_i}{r} \right] n_i dS \propto \left(\frac{U_o}{D} \right) \left(\frac{\rho_o U_o}{r} \right) (D^2) \propto \frac{U_o^2}{r}. \quad (1.16)$$

$$II : W \propto p'^2 \propto \frac{U_o^6}{r^2}, \quad (1.17)$$

$$III : W \propto p'^2 \propto \frac{U_o^4}{r^2}. \quad (1.18)$$



Figure 1.1. Photograph of Gulfstream 550 Nose Landing Gear

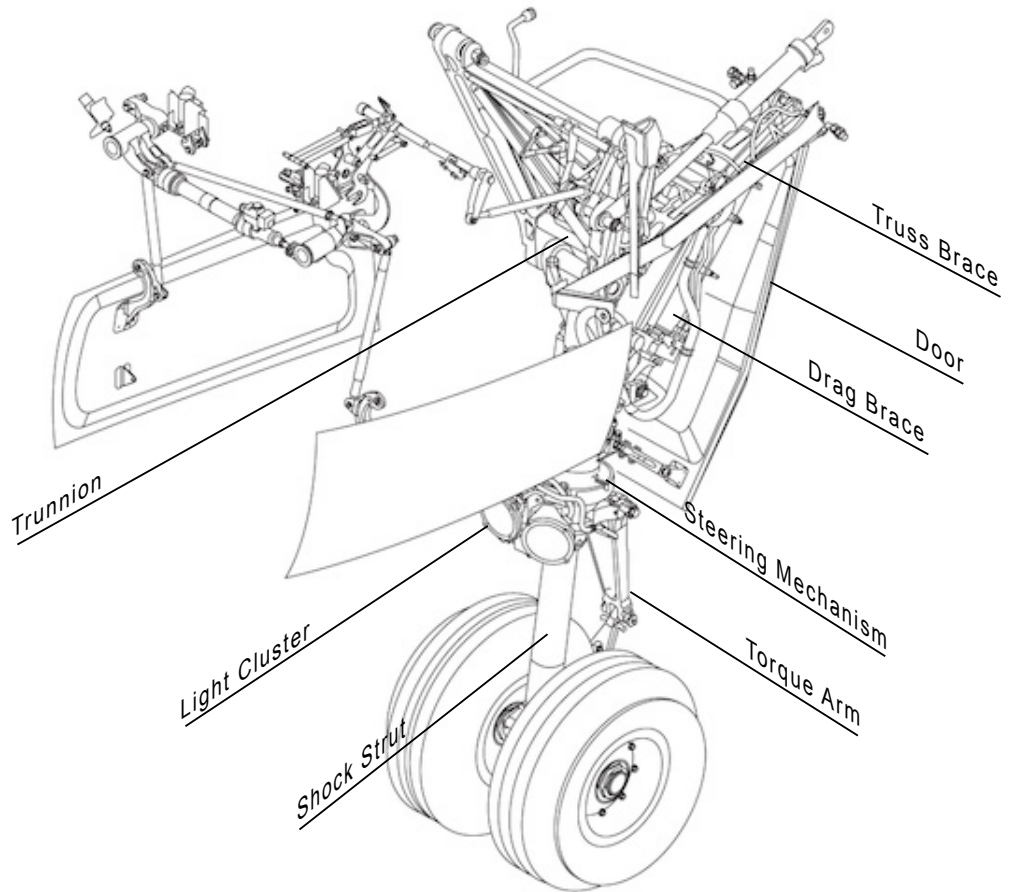


Figure 1.2. Schematic view of Gulfstream 550 Nose Landing Gear components

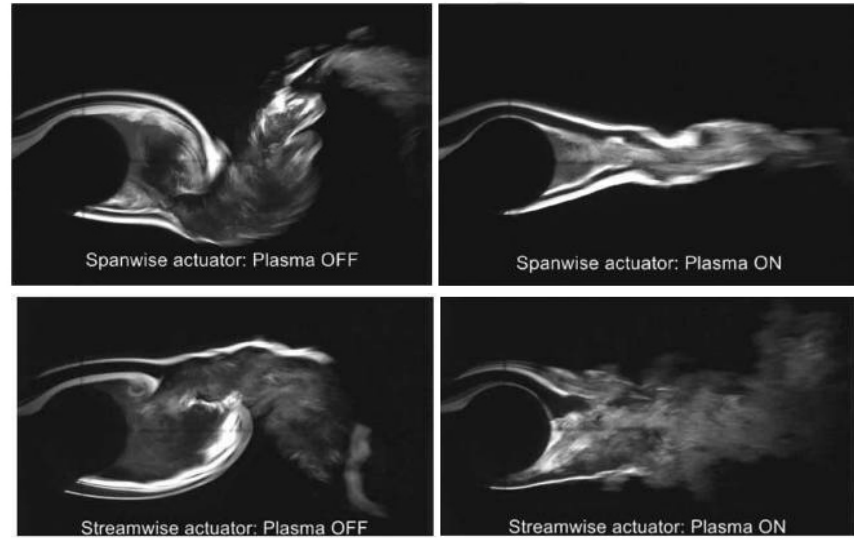


Figure 1.3. Flow Visualization of single cylinder in cross-flow with Spanwise and PSVG plasma actuators.

1.3 Landing Gear

1.3.1 Geometry

1.3.2 Noise Sources

1.4 Literature Review

1.4.1 Single Cylinder Plasma Flow Control

1.4.2 Tandem Cylinders Plasma Flow Control

1.4.3 Shock Strut-Torque Arm Assembly Plasma Flow Control

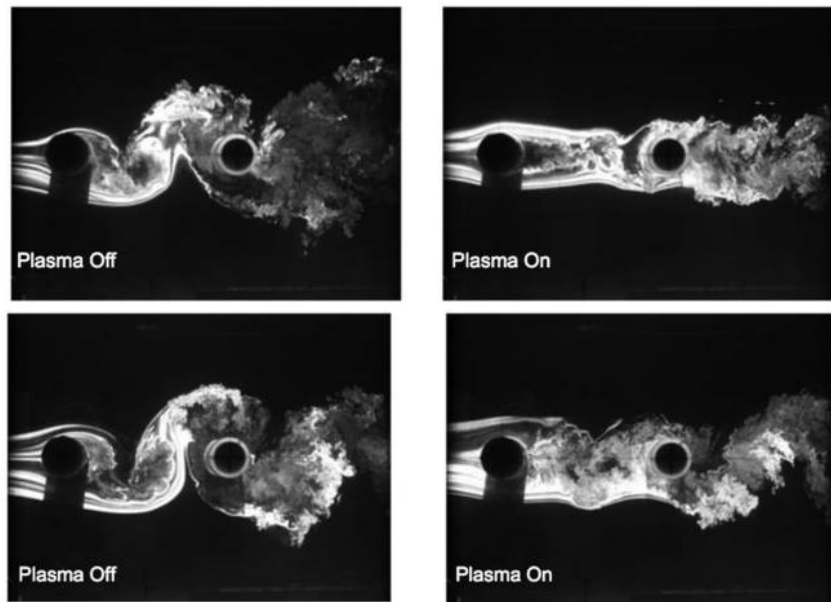


Figure 1.4. Flow Visualization of tandem cylinders in cross-flow with Spanwise and PSVG plasma actuators.

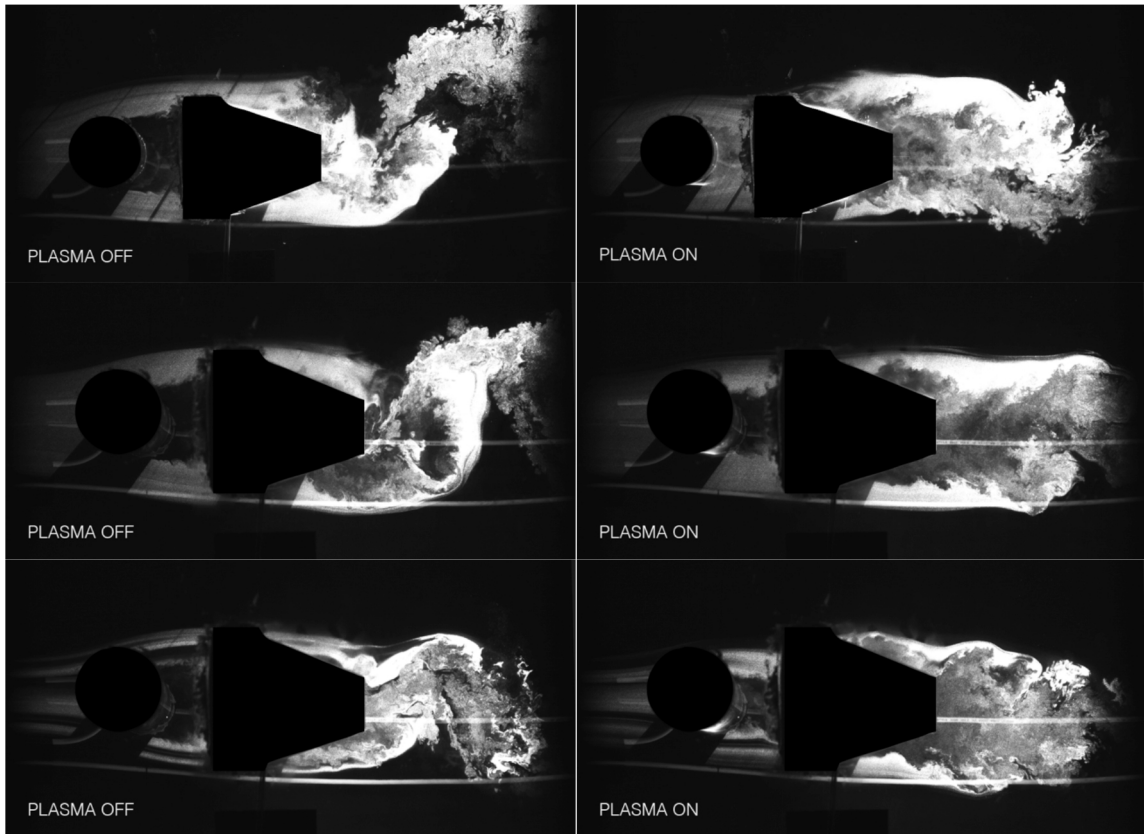


Figure 1.5. Flow Visualization of torque-arm assembly in cross-flow with Spanwise plasma actuators.

CHAPTER 2

EXPERIMENTAL APPROACH

2.1 Experimental Objective

2.2 Experimental Facility

Baseline acoustic measurements without plasma flow control were obtained in the Notre Dame Anechoic Wind Tunnel Facility (ND AWT). The ND AWT is a low-noise, open-jet acoustic wind tunnel with a free jet test section measuring 24-in-(0.610 m)-high by 24-in-(0.610 m)-wide installed in a large anechoic chamber suitable for frequencies above 100 Hz. The maximum empty test section velocity is approximately $U_\infty = 35$ m/s. The maximum safe tunnel velocity with the Notre Dame G550 Nose Landing Gear 30%-scale model (ND G550) installed is 30 m/s corresponding to a Mach number of $M_\infty = 0.1$.

Atmospheric properties such as ambient temperature and pressure were acquired using a digital thermometer and barometer. The tunnel speed is measured using a pitot-static probe installed approximately 6 in (0.154 m) from the free jet inlet centerline. From these data local sonic speed and the flow Mach number is computed.

2.3 Notre Dame G550 Nose Landing Gear Model

Acoustic measurement for two baseline landing gear model configurations were performed. The first, designated Baseline 1, consisted of the ND G550 model without the plasma fairing installed, which is shown in the photograph of Figure 2.1a. The second, designated Baseline 2, involved the ND G550 model retrofitted with a plasma



(a) Baseline 1



(b) Baseline 2

Figure 2.1. ND G550 model with and without plasma fairing installed.

fairing assembly in order to facilitate installation of dielectric barrier discharge (DBD) plasma actuators for flow control. This configuration is shown in the photograph of Figure 2.1b. None of the acoustic measurements presented in this report for both configurations involved the use of plasma flow control. Rather, the focus was on the characterization of baseline acoustics for both configurations.

2.4 Flow Visualization

2.5 Pressure Measurements

2.6 Microphone Measurements

A polar array of omnidirectional microphones was used to acquire far field noise level spectra along the length of the AWT test section. It consists of a 1/2-in ACO Model 7046 electret microphone with companion 4012 preamplifier and PS9200 power supply. A schematic illustrating the array is shown in Figure 2.2. Additionally, the array configuration relative to the G550 model is shown in the photograph of Figure 2.3. The microphone is mounted using a microphone stand so as to protrude from an acoustically treated rail by approximately 13 in (0.330 m). The total range of acoustic source-to-microphone angle spanned by the polar array is approximately $30^\circ \leq \theta \leq 150^\circ$ as referenced from the upper torque arm of the model in the downstream flow direction. As shown in Figure 2.3, the polar array is situated along the length of the free jet test section and positioned at the same height as the upper torque arm of the model, with the plane of the microphone located approximately 59 in (1.50 m) from the test section centerline.

2.7 Data Acquisition

For microphone data acquisition, a National Instruments USB-6343 DAQ was used, yielding a total of 45 available channels with 48-bit ADC. The sampling pa-

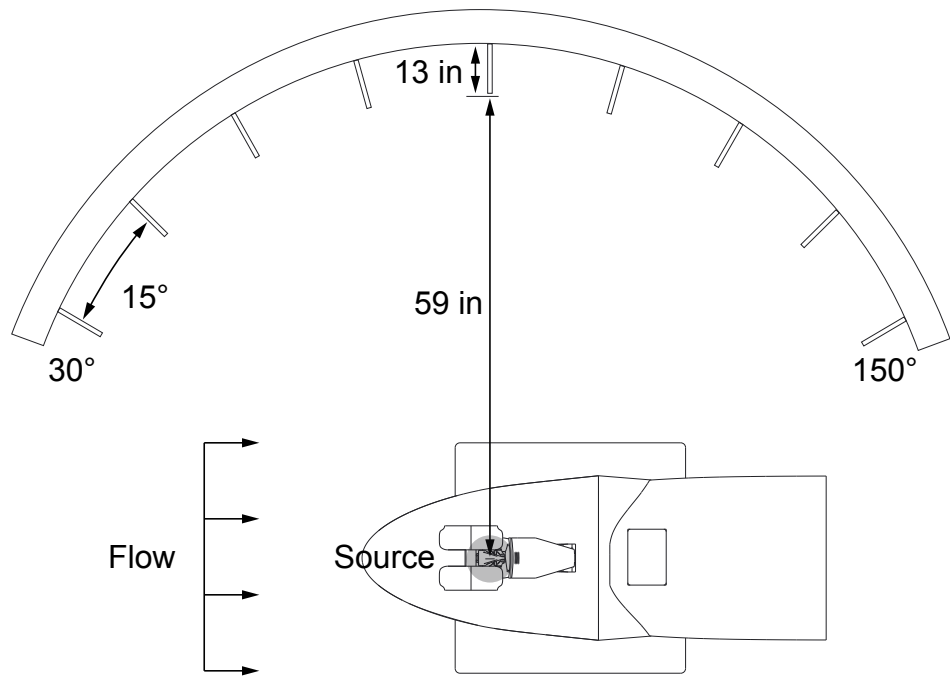


Figure 2.2. Schematic of the polar array.

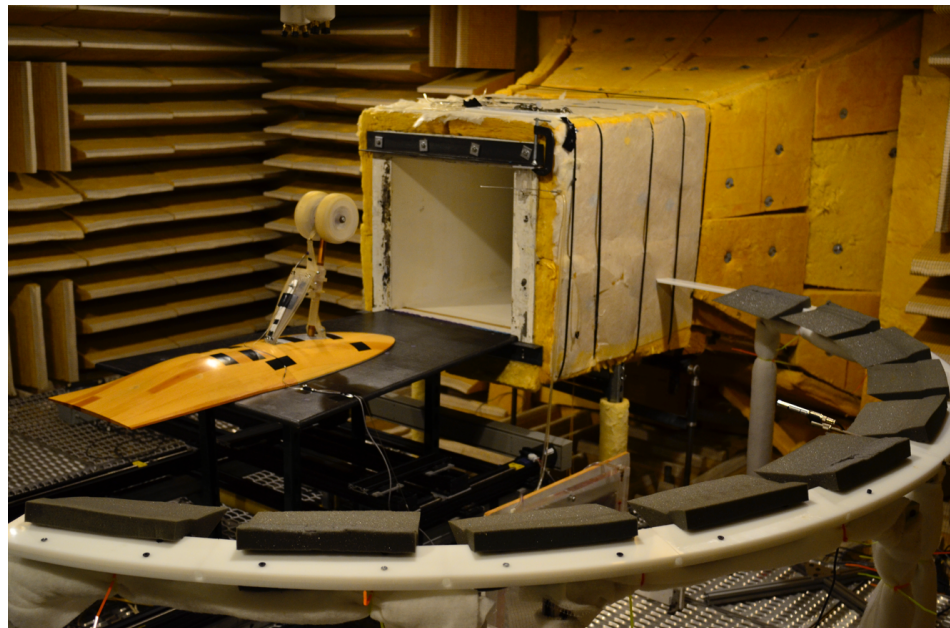


Figure 2.3. Photograph of the polar array installed in the ND AWT.

TABLE 2.1

Data acquisition parameters.

Sensors	Sampling Rate (Hz)	$\frac{Samples}{block}$	Window Function	Overlap (%)	N_{blocks}	$N_{averages}$	Acquisition Time (s)
ACO	65,536	2048	Hanning	0	960	960	30

rameters for the microphone data acquisition are listed in Table 2.1.

2.8 Current Results

2.8.1 Wind Tunnel Background Noise Characterization

It was deemed important to establish that the background noise levels in the ND AWT were sufficiently below that of the ND G550 model. To that end, measurement of noise levels for both Baseline 1 and Baseline 2 G550 configurations were compared with those obtained with the AWT tunnel running empty. Figure 2.4 presents a representative comparison of 1/3-octave band sound pressure level (SPL) spectra obtained for the Baseline 1 configurations and the empty tunnel. The figure clearly shows that the background empty tunnel noise level is several orders of magnitude below that of the ND G550, so that the effects of plasma flow control on noise production will be detectable in this facility.

2.8.2 Far field check

This section describes a procedure for verifying the far field assumption for microphone measurements.

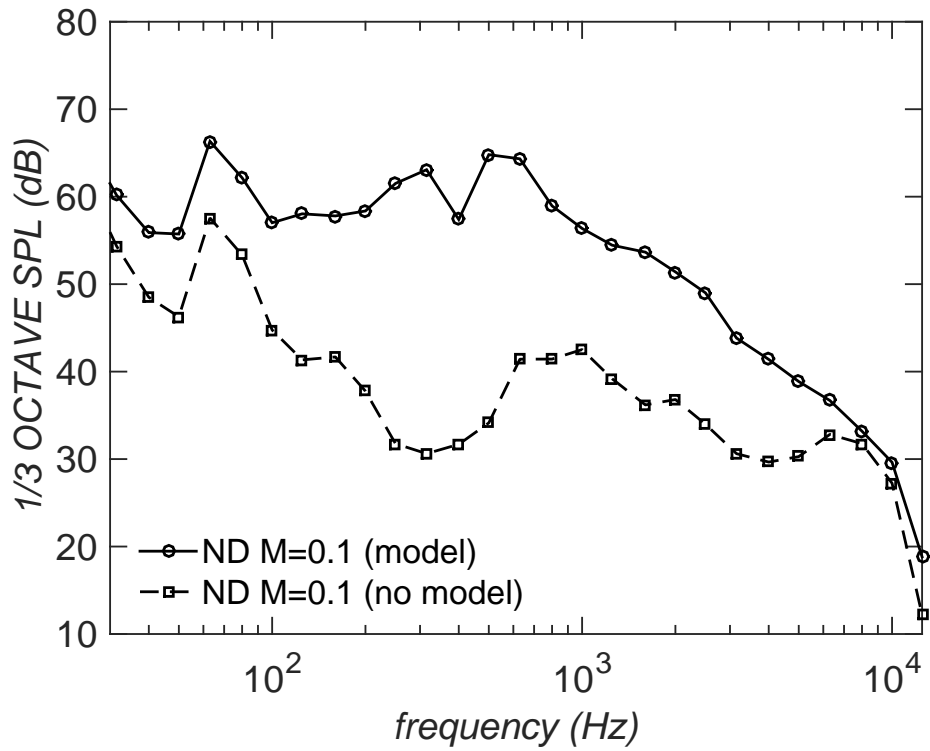


Figure 2.4. Representative far field noise level with and without Baseline 1 model installed at $\theta = 90^\circ$

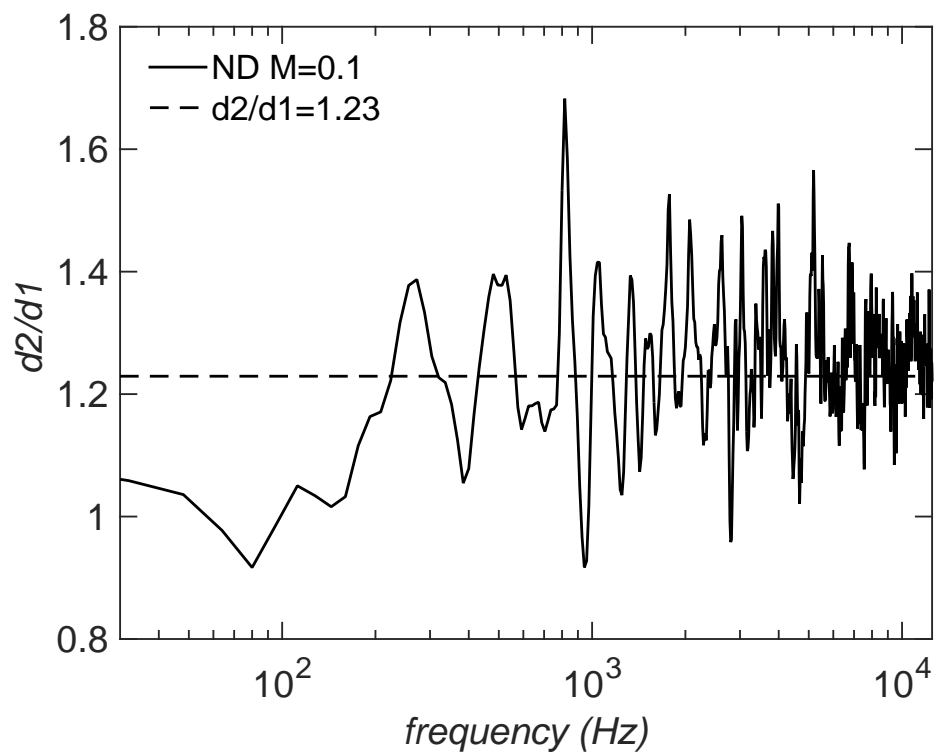


Figure 2.5. Representative far field noise level with and without Baseline 1 model installed at $\theta = 90^\circ$

2.8.3 Effects of Tripping

Previous work on the NASA G550 Nose Landing Gear (NASA G550) involved application of serrated transition strips that were applied along the length of the shock strut in order to create a turbulent boundary layer prior to separation. For consistency with this previous work, the influence of similar aerodynamic trips was explored on the ND G550 Baseline 1 model. A distributed roughness element made of standard diving board tape was fixed to the shock strut. Sample results comparing 1/3-octave band SPL spectra for the tripped and untripped cases are presented in Figure 2.6. This figure shows that there was very little influence of the trip on radiated noise. Since a trip would restrict the optimum placement of the plasma actuators, it was omitted from the model and the acoustic results that follow were obtained without tripping unless otherwise indicated.

2.8.4 Comparison with University of Florida Anechoic Flow Facility Measurements

To match the numerical simulations being performed concurrently in this study, the far field microphone distance d , was 72 in (1.83 m) array-to-model and 59 in (1.50 m) microphone-to-model. However, previous studies conducted at the University of Florida Anechoic Flow Facility (UFAFF) on the NASA G550 model were performed at a source-to-microphone distance of 48 in. In order to form a basis for comparison with acoustic results from that study, 1/3-octave band SPL spectra were obtained with the ND Baseline 1 model in the ND AWT for a source-to-microphone distance of 48 in (1.22 m). Even after accounting for the source-to-microphone distance disparity, the UFAFF experiments were performed at a freestream Mach number $M_\infty = 0.189$ and the Notre Dame experiments were performed at $M_\infty = 0.1$. The effect of disparate Mach numbers on the SPL can be accounted for by scaling the Notre Dame results via the relation,

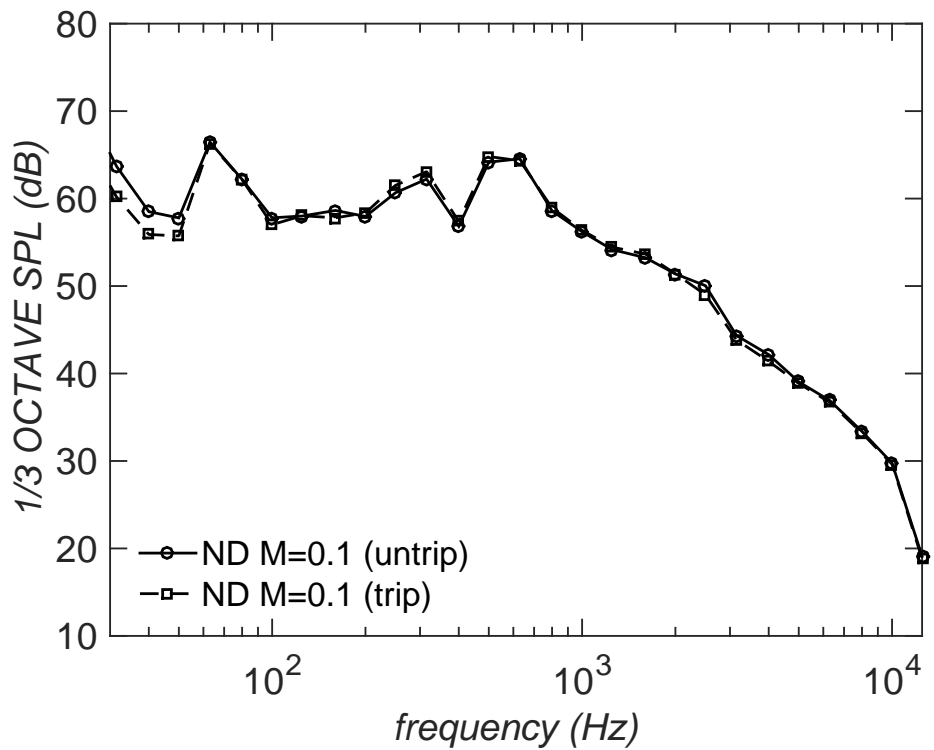


Figure 2.6. Comparison of far field noise level with and without the presence of a trip at $\theta = 90^\circ$

$$SPL_2 = SPL_1 - 10 \log \left(\frac{M_1}{M_2} \right)^6, \quad (2.1)$$

where SPL_1 and M_1 denote the ND AWT experimental values, M_2 denotes the UFAFF test Mach number (0.189) and SPL_2 represents the ND AWT sound pressure level values corrected for Mach number. Figure 2.7 compares 1/3-octave band SPL spectra obtained in both facilities for the case of $\theta = 90^\circ$. In this plot the frequency is expressed in terms of Strouhal number, $St_D = fD/U_\infty$, where length scale D is the shock strut diameter upstream of the torque arm and U_∞ is the freestream velocity. There is good collapse of the NASA G550 and ND G550 data from $0.3 \leq St_D \leq 0.6$. Below this range there is about 4-5 dB difference before the 100 Hz AWT cutoff frequency. Above this range there is significant discrepancy. The NASA G550 model is characterized by a peak near $St_D = 3$ and spectral roll-off above this peak. The ND G550 model lacks this high frequency content. The components of the ND G550 model are mostly fabricated from SLA plastic, while the NASA G550 consists of mostly aluminum and carbon fiber. To compensate for the differences in tensile strength, thickness was added to several components of the ND G550 model as shown in the CAD images in Figure 2.8. Additionally, it was necessary to construct most of the ND G550 model from plastic to facilitate the retrofitting of plasma actuators. It is possible, but by no means certain that these design modifications may play a role in the observed differences in noise spectra.

2.8.5 Baseline Sound Magnitude and Directivity

The Overall Sound Pressure Level (OASPL) is calculated by integrating the power spectral density from $100 \leq f \leq 12,500$ Hz. OASPL at each location of the polar array, $30^\circ \leq \theta \leq 150^\circ$, is given in Figure 2.11. Baseline far field 1/3-octave band spectra are reported for each location on the polar array in Figure 2.9. There is

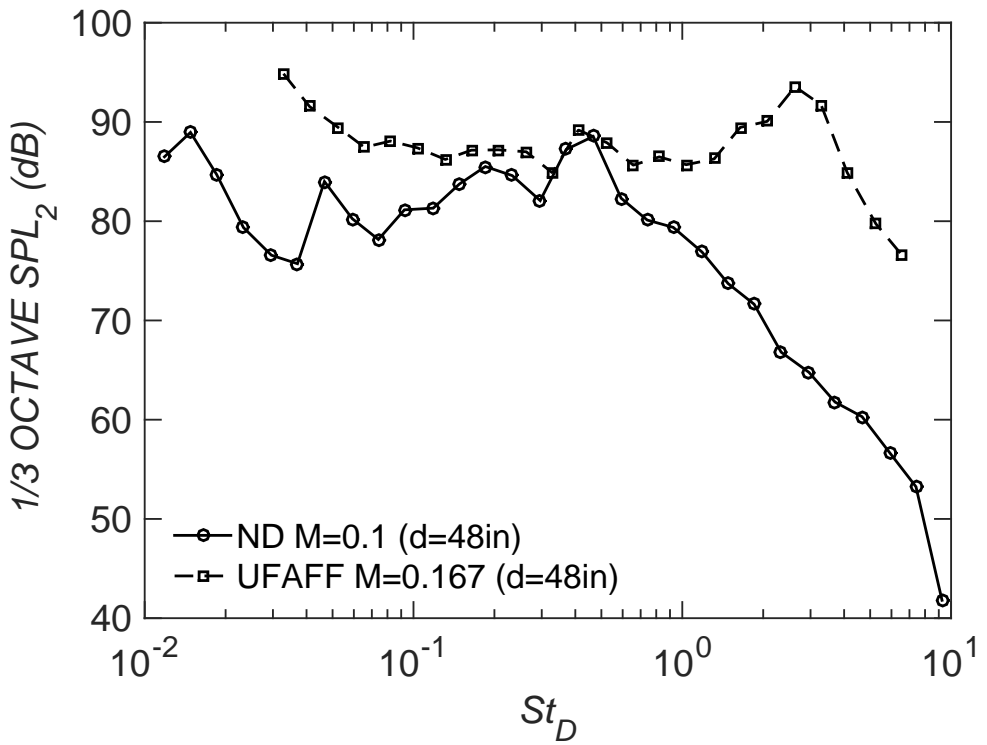


Figure 2.7. Comparison of far field noise level at UFAFF and ND AWT facilities at $\theta = 90^\circ$

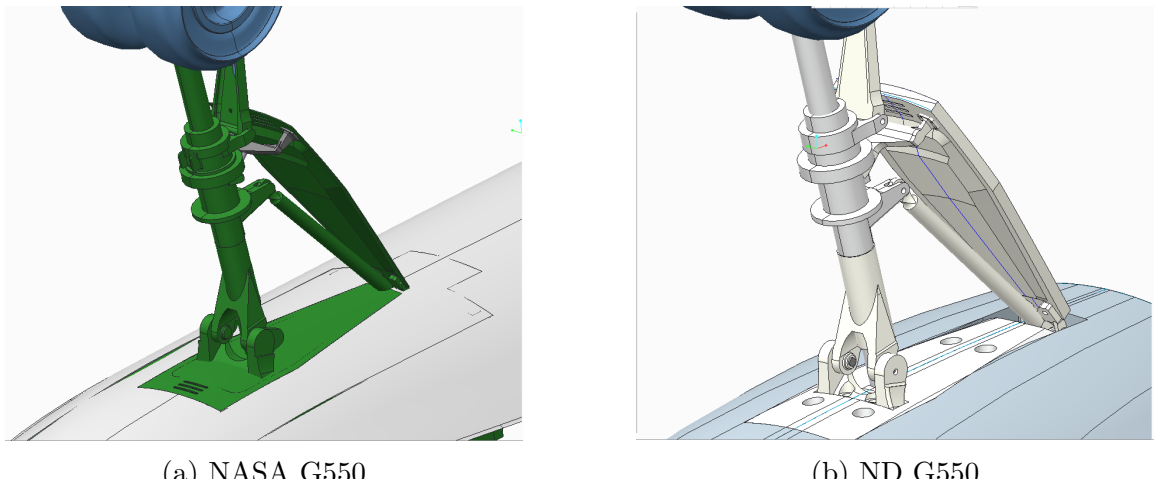


Figure 2.8. Comparison of design of the NASA G550 and ND G550 model geometries.

consistent noise reduction of about 6 dB observed at each microphone location from $100 \leq f \leq 200$ Hz. Additionally, the twin peaks at 300 Hz and 500 Hz respectively show up as one peak at 300 Hz for the $\theta = 30^\circ$ location. These spectral peaks increase in magnitude with increasing θ , for $\theta \leq 90^\circ$, and decrease in magnitude for $90^\circ < \theta \leq 150^\circ$. Similar observations were made in unsteady pressure during the Phase I study on the ND torque arm model, suggesting that these peaks are characteristic of the torque arm section of the ND G550 model. However, this will need to be substantiated with unsteady pressure data on the ND G550, which will be included in the next report. Finally, the shape of the partial directivity plot exhibits dipole-like behavior.

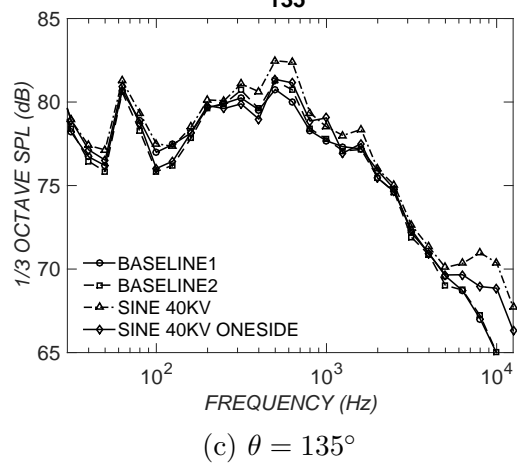
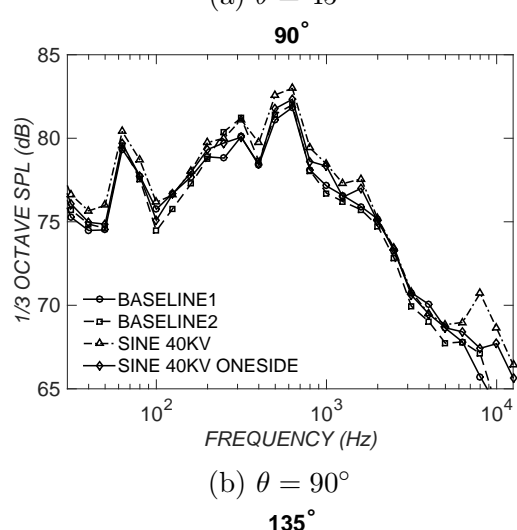
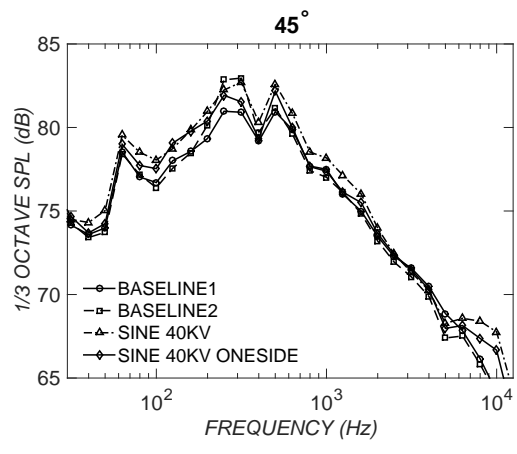


Figure 2.9. 1/3-octave band SPL

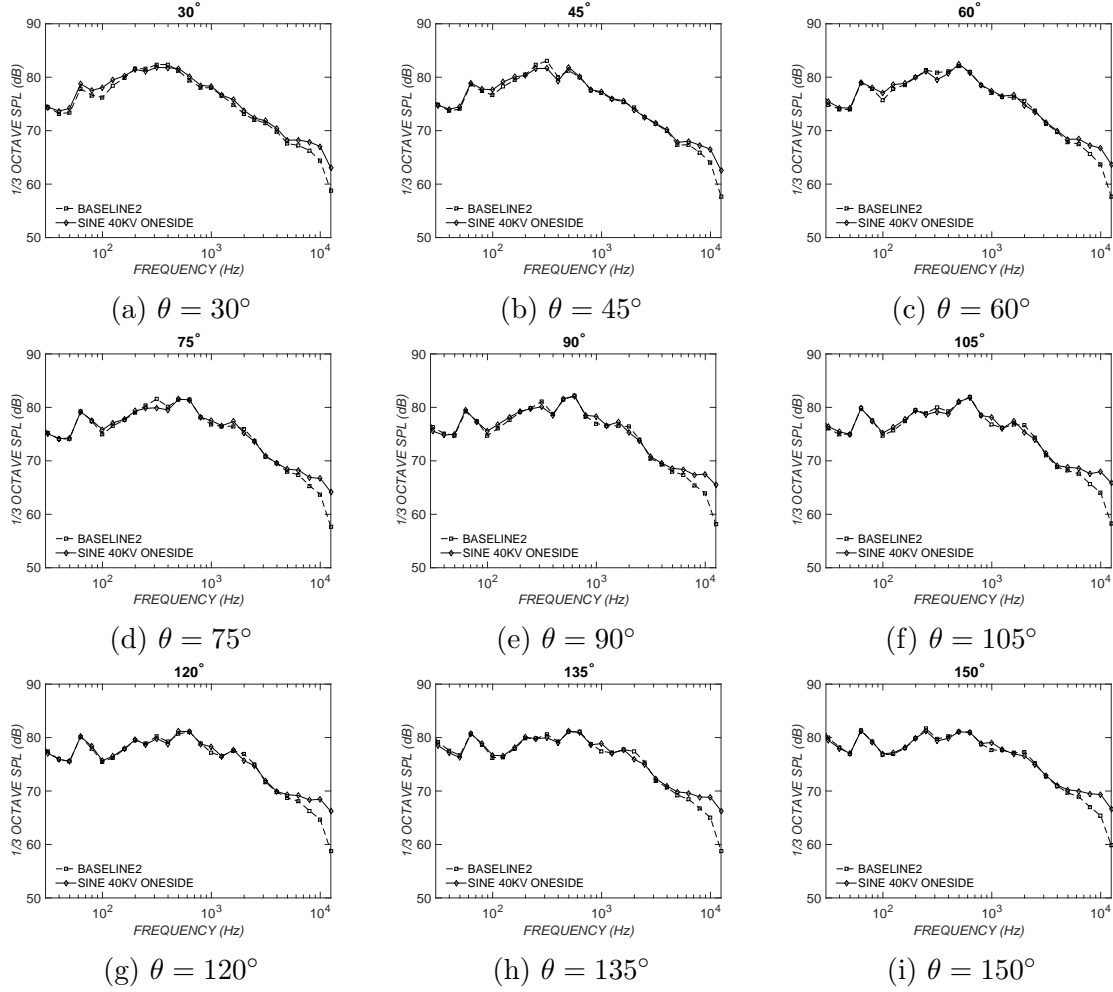


Figure 2.10. 1/3-octave band SPL

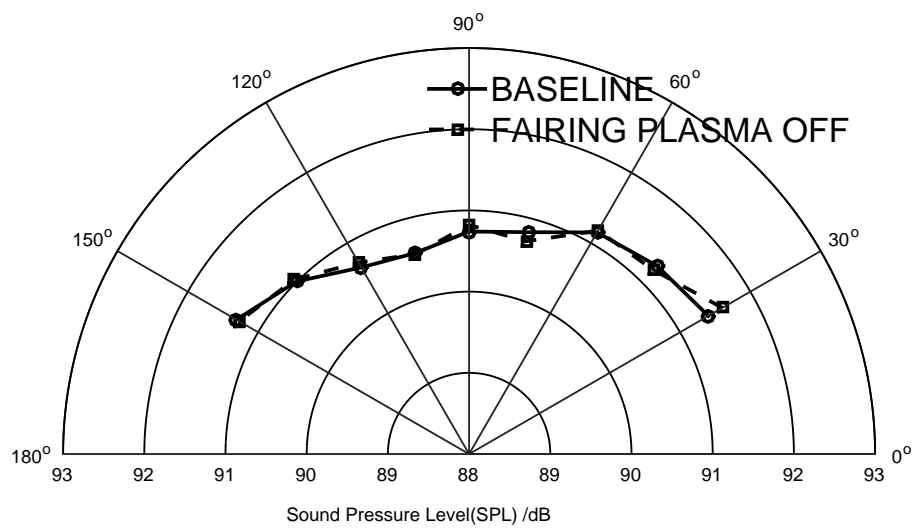


Figure 2.11. Polar plot



Figure 2.12. Landing Gear Flow Visualization

CHAPTER 3

OBJECTIVES AND FUTURE WORK

3.1 Research Objectives

3.2 Proposed Future Work

3.3 Conclusion

BIBLIOGRAPHY

1. M. S. Howe. *Theory of Vortex Sound - Lighthill's Theory*. Cambridge University Press, 2003.

This document was prepared & typeset with pdfL^AT_EX, and formatted with NDDiss2_ε classfile (v3.2013[2013/04/16]) provided by Sameer Vijay and updated by Megan Patnott.